CONCLUSION

We have analyzed excitation and emission spectra of NaI(Tl) at high Tl concentrations as a function of temperature and concentration. The main result we have obtained is the evidence for an energy transfer from dimer centers to nearby monomer centers. This evidence consists of the behavior of the quantum efficiency of the transfer luminescence versus Tl concentration, of the coalescing of monomer and transfer luminescence peak positions and half-widths at LHeT, and finally of the essentially equal value of their decay times.

ACKNOWLEDGMENTS

We would like to express our thanks to Dr. W. Beall Fowler for helpful discussions and to the Harshaw Chemical Co. for generously providing us with the crystals.

PHYSICAL REVIEW VOLUME 168, NUMBER 3 15 APRIL 1968

Lattice Vibrations of Yttrium Vanadate*

S. A. MILLER, H. H. CASPERS, AND H. E. RAST
Infrared Division, Research Department, Naval Weapons Center Corona Laboratories†
Corona, California

(Received 18 September 1967)

The lattice vibrations of YVO_4 have been analyzed group-theoretically, and symmetry coordinates for the vibrations have been constructed. The first-order Raman spectrum is reported in detail and preliminary results of infrared (IR) measurements are given. Six of the seven allowed IR-active modes and nine of the twelve allowed Raman-active modes have been observed. Symmetry assignments are given for all observed modes.

I. INTRODUCTION

YTTRIUM vanadate has recently emerged as a material of considerable interest as a host for phosphors and solid-state lasers as well as for the study of rare-earth ions in general. In this paper we present the results of an infrared and Raman study of the vibrational spectrum of YVO_4 and its interpretation in terms of symmetry coordinates in the YVO_4 lattice.

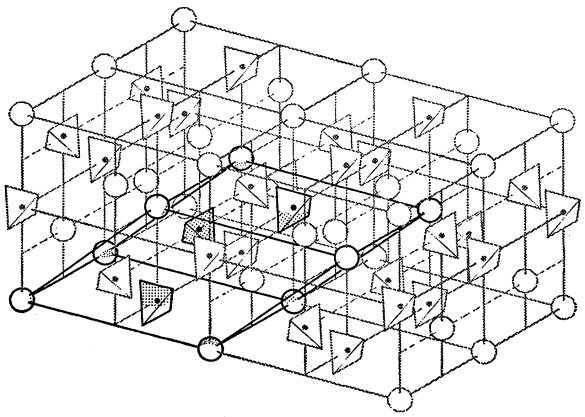

FIG. 1. The crystal structure of YVO_4. One choice for the primitive cell is shown in heavy lines with the part of each ion belonging to this cell shaded. Yttrium atoms are shown as circles and VO_4^{-3} ions as tetrahedrons.

YVO_4 crystallizes in the D_{4h}^{19} structure of zircon.[1] This structure is tetragonal with a c/a ratio of 0.883 and is not optically active. The primitive cell contains two molecules as shown schematically in Fig. 1.

A number of crystals with structure similar to YVO_4 have already been studied. In particular, we might cite Richman's Raman study[2] and Mooney and Toma's infrared work[3] on YPO_4. Analogous work on crystals of the scheelite (C_{4h}) structure has been reported by Russell and Loudon,[4] Porto and Scott,[5] and Barker.[6]

In the following sections we present a group-theoretical character analysis of the vibrational modes of YVO_4, showing how some of the lattice modes derive from the internal vibrations of the VO_4^{-3} complex. Symmetry coordinates are worked out for the allowed modes. The Raman and IR spectra of this material are described and in the final section we discuss the assignment of the observed modes to the various allowed symmetry species of the lattice.

II. GROUP THEORY

The two YVO_4 molecules per primitive cell in the D_{4h} zircon structure support $3\times2\times6=36$ modes of

* Work supported in part by the U. S. Office of Naval Research.
† Formerly Naval Ordnance Laboratory, Corona, Calif.

[1] R. W. G. Wyckoff, *Crystal Structures* (Interscience Publishers Inc., New York, 1965), 2nd ed., Vol. 3.
[2] I. Richman, J. Opt. Soc. Am. **56**, 1589 (1966).
[3] R. W. Mooney and S. Z. Toma, J. Chem. Phys. **46**, 3364 (1967).
[4] J. P. Russell and R. Loudon, Proc. Phys. Soc. (London) **85**, 1029 (1965).
[5] S. P. S. Porto and J. F. Scott, Phys. Rev. **157**, 716 (1967).
[6] A. S. Barker, Jr., Phys. Rev. **135**, A742 (1964).

vibration with $\mathbf{k}=0$ including the zero-frequency translational motion of the crystal. By applying the methods of group theory as described by Hornig[7] and by Winston and Halford,[8] one may determine the number of modes belonging to each of the allowed symmetry species of D_{4h}. One finds that the 36-dimensional representation of the full symmetry group of YVO_4 decomposes as follows into the irreducible representations of D_{4h}:

$$\Gamma_{36}=(2A_{1g}+2B_{1u})+(B_{1g}+A_{1u})+(A_{2g}+B_{2u})+(4B_{2g}+4A_{2u})+(5E_g+5E_u). \quad (1)$$

The pairs of species enclosed in parentheses derive from the same motion of the YVO_4 molecule, but for both molecules in the primitive cell the first is even and the second is odd with respect to inversion.

It has been observed that solids comprising an ionic complex such as VO_4^{-3} often exhibit modes in their vibrational spectra which are due essentially to internal vibrations of the atoms of the complex.[9] We can try to gain insight into the nature of the whole vibrational picture of YVO_4 by considering separately vibrations of the tetrahedral complex VO_4^{-3}. Here there are five atoms which support 15 modes of motion including free rotation and translation. The reducible representation of the T_d symmetry group of the complex breaks down as follows:

$$\Gamma_{15}=A_1+E+F_1+3F_2, \quad (2)$$

where F_1 is the species of pure rotation and one of the F_2's corresponds to pure translation. The normal modes of internal vibration of a five-particle tetrahedron like VO_4^{-3} have been worked out exactly and are given, for example, by Herzberg.[10] Following the usual notation we refer to the frequency of the A_1 vibration as ν_1, of the E vibration as ν_2, and of the two internal F_2 vibrations as ν_3 and ν_4. The normal modes are shown in an excellent figure in Herzberg,[11] and their frequencies have been measured in an aqueous solution of Na_3VO_4 by Siebert[12]:

$$\nu_1=870\ \text{cm}^{-1},$$
$$\nu_2=345,$$
$$\nu_3=825,$$
$$\nu_4=480.$$

In the crystal, the rotational F_1 modes and translational F_2 modes of the VO_4^{-3} complex will correspond essentially to vibrations of the VO_4^{-3} cage as a whole and will have nonzero frequencies. We shall refer to the crystal modes which involve these types of motion as external modes to contrast them with the internal modes of the VO_4^{-3} tetrahedron.

We can see what becomes of these modes by considering the reduction of the representations of T_d under the D_{2d} symmetry of the VO_4^{-3} site in the lattice: $A_1\rightarrow A_1$, $E\rightarrow A_1+B_1$, $F_1\rightarrow A_2+E$, $3F_2\rightarrow 3B_2+3E$. The doubly degenerate E mode is split and the triply degenerate F modes are partially split. Since there are two VO_4^{-3} radicals in each primitive cell, there are actually twice as many modes of each species (that is, modes in which the motions of the VO_4^{-3} complex belong to each irreducible representation of D_{2d}). These pairs of modes would be degenerate if there were no interaction between the two molecules in the primitive cell; in the crystal the degeneracy is split by an amount indicative of the coupling between the molecules.

The yttrium atoms in YVO_4 also occupy sites of D_{2d} symmetry. The z coordinate of an yttrium atom transforms as B_2 while the x and y coordinates transform as E. Therefore we need to add, for the two yttrium atoms in a primitive cell two more B_2 modes and two more E modes.

We find then that there are all together four A_1, two A_2, eight B_2, and ten E modes for which the motions of the Y^{+3} and VO_4^{-3} ions transform according to the respective irreducible representations of D_{2d}. As a final step to complete the circle we can check the correlation between the representations of D_{2d} and D_{4h} as determined at the beginning. We find, for example, that A_{1g} and B_{1u} modes of D_{4h} both correspond to A_1 modes in D_{2d}. Since A_{1g} and B_{1u} are simply related by the inversion operation, there must be equal numbers of modes of each, the A_{1g} corresponding to 180°-out-of-phase motions of the two molecules in the YVO_4 primitive cell and the B_{1u} corresponding to in-phase motions. Therefore the four A_1 modes of D_{2d} correspond to $2A_{1g}$ and $2B_{1u}$ modes in D_{4h} in agreement with (1). In a similar way we can work out the correlations between the remaining modes in D_{2d} and D_{4h}. The results of this section are all summarized in the correlation chart (Fig. 2).

III. SYMMETRY COORDINATES

As symmetry coordinates[13] for the internal modes of YVO_4 we simply take the normal modes of the VO_4^{-3} tetrahedron.[11] We do not expect these motions to be normal modes in the crystal because of perturbations due to neighboring atoms, but they do retain the correct transformation properties and would therefore be useful as a starting point in a force-constant calculation of the vibrational spectrum.

Figure 3 shows the symmetry coordinates for the internal vibrations. Only one of the VO_4^{-3} ions is shown for each species. In the primitive cell, the u modes have both VO_4^{-3} ions vibrating in phase as shown; the g

[7] D. F. Hornig, J. Chem. Phys. **16**, 1063 (1948).
[8] H. Winston and R. S. Halford, J. Chem. Phys. **17**, 607 (1949).
[9] See, for example, A. S. Davydov, *Theory of Molecular Excitons* (McGraw-Hill Book Co., New York, 1962).
[10] G. Herzberg, *Molecular Spectra and Molecular Structure* (D. Van Nostrand Co., Inc., New York, 1945), Vol. II, pp. 99ff.
[11] G. Herzberg, *Molecular Spectra and Molecular Structure* (D. Van Nostrand Co., Inc., New York, 1945), p. 100.
[12] H. Siebert, Z. Anorg. Allgem. Chem. **275**, 225 (1954).
[13] E. B. Wilson, J. C. Decius and P. C. Cross, *Molecular Vibrations* (McGraw-Hill Book Co., New York, 1955), pp. 117ff.

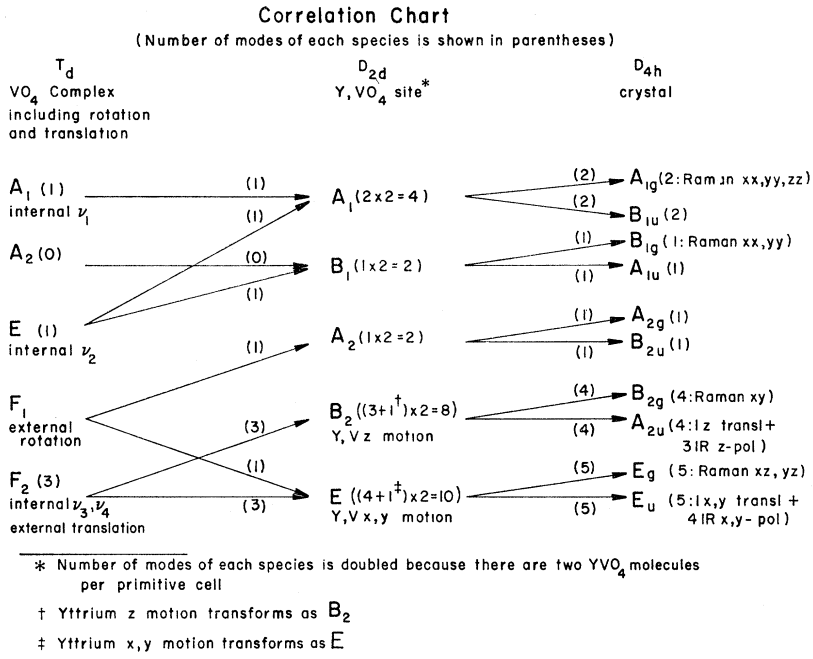

FIG. 2. Correlation chart for symmetry species of the T_d group of the VO_4^{-3} free ion, the D_{2d} group of the Y^{+3} and VO_4^{-3} sites in the YVO_4 crystal, and the D_{4h} group of the whole crystal.

modes have one ion displaced as shown and the other with all arrows reversed.

Under the D_{2d} symmetry of the yttrium and vanadium sites, the z and x, y coordinates transform accord-

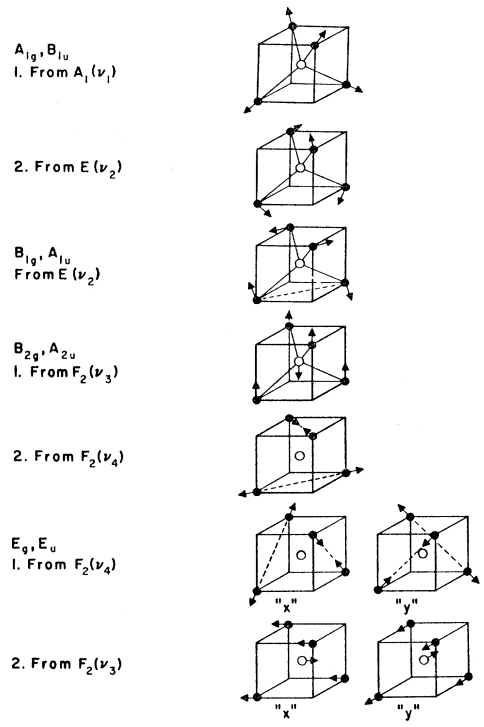

FIG. 3. Symmetry coordinates for the internal modes in YVO_4. Motions are shown for only one of the VO_4^{-3} ions in the primitive cell. *Ungerade* modes have both ions executing the same motion in phase; *gerade* modes are 180° out of phase. ●, oxygen; ○, vanadium.

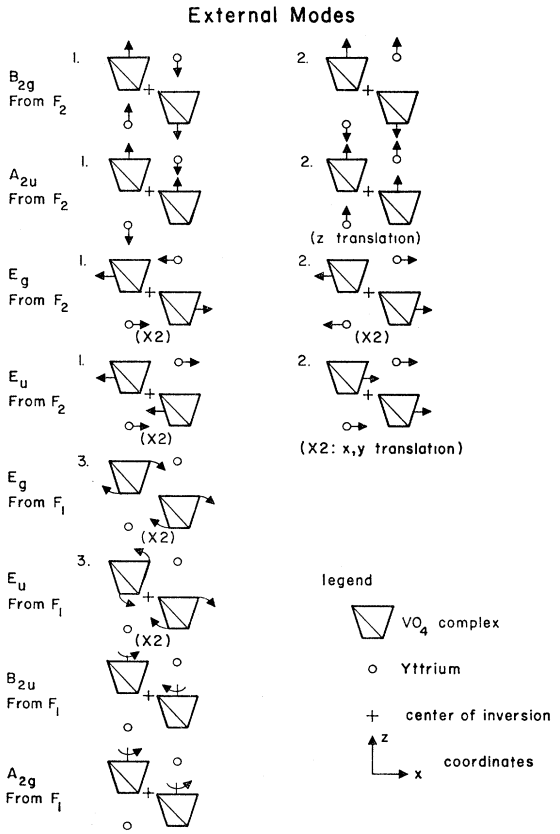

FIG. 4. Symmetry coordinates for the external modes in YVO_4. For the doubly degenerate E modes, only motion in the xz plane is shown; similar motions in the yz plane complete the bases for the E modes.

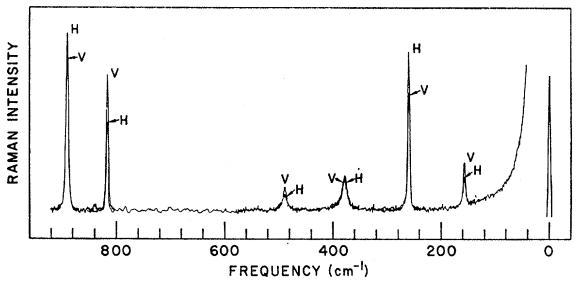

FIG. 5. Raman spectrum of YVO_4 single crystal at room temperature: (V) α_{xy}, (H) α_{yy}.

ing to B_2 and E, respectively. Group theory assures us then that in all of the modes derived from the other D_{2d} species neither the yttrium nor the vanadium atoms can move. This prediction is confirmed in our choices for the A_{1g}, B_{1u}, B_{1g}, and A_{1u} symmetry coordinates. It happens that in the $F_2(\nu_4)$ vibration of VO_4^{-3} the vanadium does not move although its motion is not excluded by symmetry. In the crystal, the internal B_{2g}, A_{2u}, E_g, and E_u modes, which are derived from the F_2 mode, may involve the motion of the yttrium and vanadium atoms even though in our choices of symmetry coordinates they do not.

The external vibrations of the crystal comprise the A_{2g} and B_{2u} modes, two each of the B_{2g} and A_{2u} modes, and three each of the E_g and E_u modes. The external B_{2g} and A_{2u} modes derive from the z part of the F_2 translational mode of VO_4^{-3} via B_2 in D_{2d}. Symmetry coordinates for these species are therefore, respectively, out-of-phase and in-phase displacements in the z direction of the two VO_4^{-3} cages and the two yttrium atoms in the primitive cell. Similarly, two of the external E_g and E_u modes may be represented by displacements parallel to the x, y plane. The A_{2g} and B_{2u} modes derive from the F_1 rotational modes in T_d via A_2 in D_{2d}. No motion of the yttrium or vanadium is permitted by symmetry, so we conclude that A_{2g} and B_{2u} are, respectively, out-of-phase and in-phase rotations of the VO_4^{-3} cages about the z axis. The remaining E_g and E_u modes are rotations of the VO_4^{-3} cage about axes in the x, y plane. Symmetry coordinates for the external modes are shown in Fig. 4.

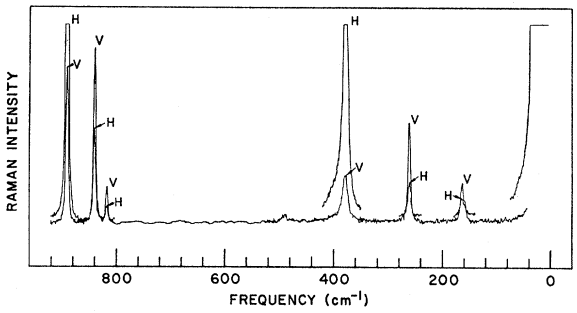

FIG. 6. Raman spectrum of YVO_4 single crystal at room temperature: (V) α_{yz}, (H) α_{zz}.

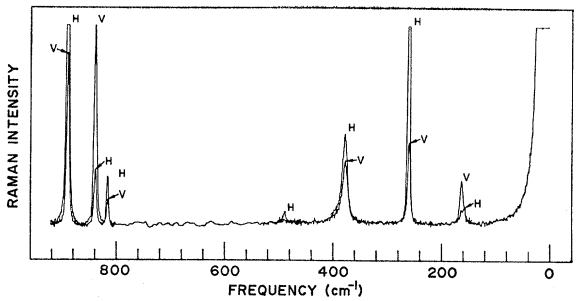

FIG. 7. Raman spectrum of YVO_4 single crystal at room temperature: (V) α_{xz}, (H) α_{xx}.

IV. RAMAN AND IR SPECTRA

Raman and IR measurements were made on several samples of YVO_4 procured from Vinor Laboratories. These single crystals were of excellent optical quality. They were oriented by x ray, and cut and polished with faces perpendicular to each of the crystal axes and at several intermediate angles. Some of the samples were doped with small amounts of neodymium and some with europium, but we do not expect any significant effect on the lattice vibrations due to these impurities.

The Raman measurements were made on a Cary Model 81 spectrophotometer using a 50-mW helium-neon laser source. Room-temperature spectra were taken at different polarizations and orientations so that all independent components of the Raman polarizability tensor were displayed. Figure 5 shows spectra contrasting α_{xy} and α_{yy}, Fig. 6 contrasts α_{yz} and α_{zz}, and Fig. 7, α_{zx} and α_{xx}. Each spectrum was taken by scanning the monochromator with a particular crystal orientation and polarization of the incident laser beam and then rotating the beam polarization by 90°, backing up the monochromator and chart, and rescanning the lines, making use of the fact that on the Cary instrument the chart and monochromator are directly coupled. Table I gives the frequencies and polarizations of the observed Raman lines. Figure 8 shows five spectra made by retracting the lines with the crystal rotated about the c axis in five different positions, beginning with an orientation measuring α_{xx}.

Although the polarization of the spectra is not complete due to imperfect orientation of the samples, nevertheless the polarization of most of the lines is

TABLE I. Frequencies and polarizations of observed Raman lines in YVO_4 at room temperature.

Frequency (cm^{-1})	Polarization
157	xy
162	yz,zx
260	xx,yy,yz
379	zz
489	xy
817	xy
840	yz,zx
891	zz,xx

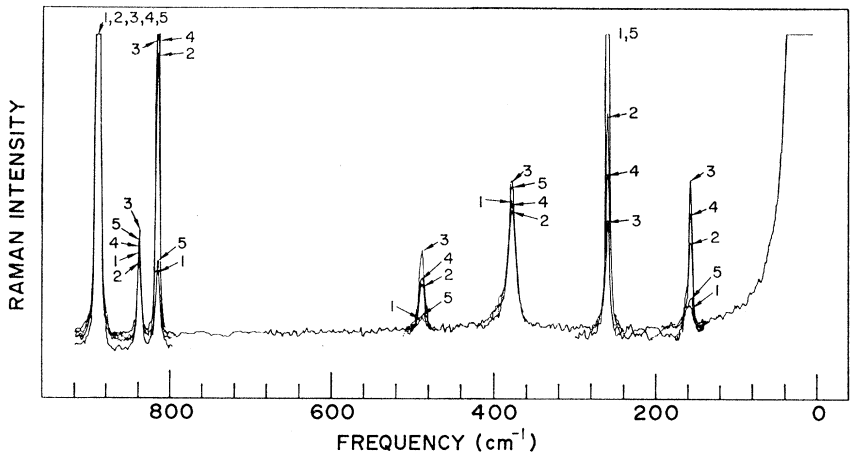

FIG. 8. Raman spectrum of YVO_4 single crystal at room temperature. Incident and scattered light are polarized in the crystal xy plane and propagate along a line in the xy plane which makes an angle θ with the crystal x axis: (1) $\theta=0°$, (2) $\theta=30°$, (3) $\theta=45°$, (4) $\theta=60°$, (5) $\theta=90°$.

unambiguous. An exception is the line at 260 cm^{-1}, which appears in the xx and yy polarizations but is also strong in the yz and zx polarizations. Referring to the correlation chart (Fig. 2), these polarizations are incompatible. However, it is possible that two or more lines of different symmetry fall at this frequency. A small shift is in fact noticeable in Figs. 5 and 7 between the polarizations shown.

Infrared spectra of YVO_4 were obtained by measuring the emittance of oriented samples over a wavelength range from 4 to 125 μ. A complete description of these measurements will be published elsewhere, so that only a brief outline of the results is given here. Spectra were taken at 4 and 77°K and showed essentially the same features. Since the emittance E, the transmittance T, and the reflectance R are related by

$$E+T+R=1, \tag{3}$$

an emittance measurement gives the same information as a reflectance measurement in regions where the sample is opaque. In YVO_4 there is some transmission at wavelengths below about 8 μ, so separate corrections were applied to the data in this region.

Two spectra were taken in each wavelength range, one with the crystal c axis perpendicular to the sample face and one with the c axis lying in the face. The perpendicular spectra show only x,y polarized vibrations; the parallel spectra show all polarizations. By subtracting, it is possible to separate the two polarizations. A least-squares fit to a set of classical oscillators was applied to the observed bands. The results are given in Table II.

TABLE II. Frequencies and polarizations of observed IR emittance bands in YVO_4 at 77 and 4.2°K.

Frequency (cm^{-1})	Polarization
196	x,y
261	x,y
310[a]	x,y
310	z
455	z
788	x,y
803	z

[a] Probably not fundamental.

V. ASSIGNMENTS AND DISCUSSION

If the crystal-binding forces are not too large compared with the binding forces in the VO_4^{-3} ion, then the frequencies of the internal lattice modes ought to be fairly close to the frequencies of the free-ion modes. Furthermore, for the same reason, the external modes, involving essentially motion of the whole, relatively massive, VO_4^{-3} cage, ought to lie at generally lower frequencies than the internal modes. In assigning symmetry species to the observed Raman and IR lines, we first look for lines of the proper polarization in the neighborhood of the free-ion frequencies. For example, the free-ion ν_1 vibration at 870 cm^{-1} gives rise to a single Raman-active mode of A_{1g} symmetry, characterized by a strong zz polarization. The Raman line at 891 cm^{-1} is undoubtedly the $A_{1g}(\nu_1)$ vibration. Similarly, the free-ion ν_3 vibration at 825 cm^{-1} gives rise to Raman-active modes of $B_{2g}(xy)$ and $E_g(yz,zx)$ symmetry which surely are the lines observed at 817 and 840 cm^{-1}, respectively. The ν_3 vibration also produces two IR-active modes of $A_{2u}(z)$ and $E_u(x,y)$ symmetry which must be the two bands barely resolved at about 13 μ in the x-, y- and x, y, z-polarized emittance spectra. Proceeding in this way, the internal mode assignments listed in Table III were established.

The spectrum shown in Fig. 8 was useful in verifying some of the assignments. Upon rotation of the crystal through an angle θ about its c axis, the component $\alpha_{x'x'}$ of the Raman polarizability tensor, measured in the rotated coordinate system, can be expressed in terms of the components of α in the unrotated coordinate system as follows:

$$\alpha_{x'y'}=\alpha_{xx}\cos^2\theta+\alpha_{yy}\sin^2\theta+2\alpha_{xy}\sin\theta\cos\theta. \tag{4}$$

Thus, for an A_{1g} mode, for which $\alpha_{xx}=\alpha_{yy}$ and $\alpha_{xy}=0$, the polarizability is unchanged upon rotation. For a B_{1g} mode, $\alpha_{xx}=-\alpha_{yy}$ and $\alpha_{xy}=0$, so $\alpha_{x'x'}=\alpha_{xx}\cos 2\theta$ and the polarizability has maxima at 0° and 90°. For a B_{2g} mode $\alpha_{xx}=\alpha_{yy}=0$ so $\alpha_{x'x'}=\alpha_{xy}\sin 2\theta$ which has a peak at $\theta=45°$. The other components of α are unaffected by rotation about the z axis. Referring to Fig. 8 it is now easy to verify that the modes at 157, 489, and 817 cm^{-1} are B_{2g} modes because they have pronounced peaks at $\theta=45°$. Similarly, the mode at 260 cm^{-1} must be B_{1g} because of the peaks at 0° and 90°; the fact that this line does not go to zero at $\theta=45°$ suggests that there may be another mode of different symmetry at nearly the same frequency, supporting our earlier conclusion. The lines at 379, 840, and 891 cm^{-1} are essentially unchanged with rotation of the crystal, so they must be due to A_{1g} or E_g modes, again confirming the assignments in Table III.

Among the assignments in Table III, three allowed Raman lines are missing: an E_g mode associated with the VO_4^{-3} ν_4 vibration, and a B_{2g} and an E_g external mode. The Raman spectra were carried as low as 25 cm^{-1}, so that either the missing lines must lie below this frequency or they must be much weaker than the rest of the lines. Looking at the results of Porto and Scott[5] on $CaWO_4$, we see many very weak lines due to external modes but no line below 84 cm^{-1}, and therefore we conclude that we simply missed some of the weakest lines.

It should be pointed out that there is a certain degree of arbitrariness in our choice of assignments for the external modes. Without a full force-constant calculation we have no real reason for selecting one line over another of the same symmetry as belonging to a particular mode. We have followed Porto and Scott's choice in assigning the higher-frequency lines to the modes originating with rotational motion of the VO_4^{-3} ions. This choice is consistent with some earlier results on LiOH in which the rotational modes were actually shown to lie higher by substituting deuterium for the hydrogen and observing the frequency shift.[14] One might suppose that Porto and Scott's work on the scheelites $CaWO_4$ and $CaMoO_4$ should give a clue to the assignments, since the rotational external modes ought to be less affected by the difference in mass between tungsten and molybdenum than the translational modes. Unfortunately, the data are ambiguous on this point, with many of the corresponding lines differing in frequency by only a few wave numbers.

[14] R. A. Buchanan, E. L. Kinsey, and H. H. Caspers, J. Chem. Phys. **36**, 2665 (1962).

TABLE III. Mode and symmetry assignments of Raman and IR spectra of YVO_4.

Mode type	Sym. species	Assigned freq. (cm^{-1})
	Internal modes	
ν_1 (870 cm^{-1})	A_{1g}	891 Raman
	B_{1u}	inactive
ν_2 (345 cm^{-1})	A_{1g}	379 Raman
	B_{1u}	inactive
	B_{1g}	260+ Raman
	A_{1u}	inactive
ν_3 (825 cm^{-1})	B_{2g}	817 Raman
	A_{2u}	803 IR z pol.
	E_g	840 Raman
	E_u	788 IR x, y pol.
ν_4 (480 cm^{-1})	A_{2u}	455 IR z pol.
	B_{2g}	489 Raman
	E_g	missing
	E_u	missing
	External modes	
Rotation	E_g	missing
	E_u	261 IR x, y pol.
	A_{2g}	inactive
	B_{2u}	inactive
Translation	B_{2g}	157 Raman
	B_{2g}	missing
	E_g	162 Raman
	E_g	260− Raman
	A_{2u}	310 IR z pol.
	E_u	196 IR x, y pol.

ACKNOWLEDGMENTS

We would like to thank a number of people who have assisted with the work reported here. Dr. H. Haber and Cary Instruments have been most cooperative in making time available on a Cary Model 81 Raman instrument. J. Bernstein and Dr. D. Stierwalt made the IR measurements and D. Smith accomplished the classical oscillator fit.